ELSEVIER

Polymer 42 (2001) 9723–9728

polymer

www.elsevier.com/locate/polymer

Positron annihilation and phase separation phenomena in polyurethane crosslinked coatings with different polyether segments

G. Consolati[a], M. Levi[b,*], S. Turri[c]

[a]Dipartimento di Fisica, Istituto Nazionale per la Fisica della Materia, Politecnico di Milano, Piazza Leonardo da Vinci 32, I-20133 Milano, Italy
[b]Dipartimento di Chimica Industriale e Ingegneria Chimica “G. Natta”, Politecnico di Milano, Piazza Leonardo da Vinci 32, I-20133 Milano, Italy
[c]Centro Ricerche e Sviluppo Ausimont S.p.A., Via S. Pietro 50/a, 20021 Bollate (MI), Italy

Received 26 February 2001; received in revised form 29 June 2001; accepted 12 July 2001

Abstract

Eight model polyurethane crosslinked coatings were obtained from different compositions of polyisocyanurates of hexamethylenediisocyanate (HDI) and isophoronediisocyanate (IPDI) with polypropylenglycol (PPG) and perfluoropolyether macrodiols (PFPE), both having M_n 1000. The polyurethanes were characterized by Differential Scanning Calorimetry (DSC) and Positron Annihilation Spectroscopy (PAS). The DSC analysis showed that PPG based polyurethanes are monophasic materials having one glass transition temperature T_g increasing with the density of crosslinking and related to the T_g of the starting polyisocyanurate. On the other hand PFPE containing polyurethanes are polyphasic with segregation of fluorinated moiety and presence of urethane phases with highly diversified T_g values. It is found that PAS is sensitive to the phase segregation; furthermore, *ortho*-positronium lifetimes are correlated to the T_g. From the analysis of PAS spectra the size distributions of the nanoholes forming the free volume was obtained.

Keywords: Polyurethane; Positron annihilation; Phase separation

1. Introduction

Polyurethane coatings are used extensively as barrier anticorrosion materials in several industrial applications. They are hard-soft type polymers where the soft segment is generally polyether or polyester, and the hard domains are given by bi or polyfunctional isocyanates [1]. Fluorinated polyurethane coatings based on perfluoropolyether (PFPE) soft segments were described in the recent literature [2]. These polymers are characterized by outstanding chemical resistance, UV-light stability and low surface energy.

In this work some model polyurethane coatings based on different fluorinated and non fluorinated polyether soft segments are described and analysed. These polyurethanes are essentially made by addition of polyether polyols with two types of cyclic polyisocyanurates, followed by crosslinking through classical urethane or urea chemistry. The resulting, three-dimensional networks are therefore highly diversified in terms of glass transition temperature (T_g), composition and density of crosslinking. These features can be investigated by means of thermal analysis (DSC), which is a fundamental technique in order to macroscopically characterize polymer structures. Since the same features influence the free volume, that is, the interchain free space available for the movements of segments of a macromolecule, it follows that a technique able to monitor the nanoholes volume will allow a microscopic interpretation of the properties of the investigated polymers, which can complement the results supplied by the thermal analysis. In our work we used positron annihilation lifetime spectroscopy; indeed, this relatively simple technique can probe the properties of the free volume holes in a non-destructive way [3]. It is based on the fact that the unstable positron–electron system, positronium (Ps), is repelled from the ionic cores of the atoms and tends to localise into the nanohole volumes; its lifetime can be related to the typical size of the holes through a semiempirical equation [4]. Therefore, it is possible to obtain the characteristic dimensions of the nanoholes by studying the Ps annihilation features in the polymer. In the following we will show correlations among thermal transitions, phase segregation phenomena and free volume hole properties of the various polymers.

---

* Corresponding author. Fax: +39-2-70638-173.
E-mail address: marinella.levi@polimi.it (M. Levi).

0032-3861/01/$ - see front matter © 2001 Elsevier Science Ltd. All rights reserved.
PII: S0032-3861(01)00515-8

2. Experimental

2.1. Materials

The polyisocyanurates (cyclic trimers) of 1,6-hexamethylenediisocyanate HDI (Tolonate HDT-LV, Rhodia) and of isophorone diisocyanate IPDI (Vestanat T1890, Huls) were used as received. Their NCO content was controlled by chemical titration according to the classical dibutylamine/HCl method [5].

Polypropyleneglycol PPG (M_n 1000, Aldrich): $H(OCH_2CHCH_3)_nOH$ and dimethylol terminated perfluoropolyethers PFPE (Fomblin® ZDOL, Ausimont) having the following structure:

$HOCH_2CF_2O(CF_2CF_2O)_p(CF_2O)_qCF_2CH_2OH$

with $p/q = 2.2$

were dried in vacuo (70°C, 10^{-1} mm Hg, 4 h) before use. The OH equivalent weight of macroglycols was determined by chemical titration with the acetic anhydride method or, in case of PFPE, by end group analysis with ^{19}F-NMR spectroscopy [6]. The catalyst dibutyl tin dilaurate DBTDL (Aldrich) was used as received.

2.2. Coating preparation

The preparation of the partially fluorinated coatings is described in detail elsewhere [2]. The non-fluorinated coatings were prepared in the same manner using PPG instead of PFPE diol. As a general procedure in the first step a polyisocyanic prepolymer was formed by addition of the polyether glycol (PPG or PFPE) to a solution of the isocyanurate trimer in anhydrous butyl acetate (final solid content 60% w/w) at 100°C, using an excess of isocyanate equivalents (NCO/OH = 3). The NCO content of the final prepolymer was controlled by chemical titration (2–4 h).

The polymeric coatings were successively prepared according to two different crosslinking mechanisms. In the former case, the prepolymer solutions were catalyzed with DBTDL (0.3% w/w on solid content), bar-applied on glass panels and self-crosslinked by exposure to atmospheric moisture at 90°C for 48–72 h, obtaining a series of four different monocomponent 'moisture-cured' (MC) coatings. In the latter case, the prepolymer solutions were added to the corresponding macroglycol in the amount needed to reach an overall OH/NCO equivalent ratio = 1. The mixtures were then catalyzed with DBTDL (0.1% w/w on solid), bar applied on glass panels and crosslinked at 90°C for 24 h, obtaining a range of four different bicomponent polyurethane coatings.

The end of the crosslinking reaction was in any case confirmed by FT-IR spectroscopy, checking the disappearance of the free NCO bands at 2270 cm^{-1}.

The crosslinked polymer films (thickness 100–300 μm) were peeled off for the following characterizations.

2.3. Differential scanning calorimetry (DSC).

Thermal transitions and heat capacity changes ΔC_p of macromers and crosslinked polyurethanes were determined by DSC with a Perkin–Elmer DSC 2 instrument (indium and n-hexane calibrated), with heating runs from 293 to 443 K and cooling runs from 293 and 113 K, at a heating/cooling rate of 20 K min^{-1}. The glass transition temperature T_g was evaluated as transition midpoint of the trace.

2.4. Positron lifetime spectroscopy

The positron source consisted of a droplet of ^{22}Na from a carrier-free neutral solution (activity: 0.3 MBq), dried on two identical Kapton foils (thickness 1.08 mg cm^{-2}), which were afterwards glued together. The source was inserted within two identical samples in a typical 'sandwich' configuration; each sample was formed by stacking several layers of the same film in order to reach a thickness sufficient to stop all the injected positrons (170 mg cm^{-2} [7]). The structure was then pressed in order to eliminate air gaps between two subsequent layers. In a preliminary study concerning the PFPE + HDI bicomponent two thick samples (1 mm each) were prepared, in order to observe possible differences with respect to the multilayered samples; however, the timing spectra resulted identical, within the errors. Therefore, we used thin films, owing to the simpler preparation procedure. Positron annihilation lifetime spectra were collected through a conventional fast–fast coincidence set-up: the γ rays corresponding to the emission of the positron ('start') and to the annihilation event ('stop') were detected by two NE111 25×25 mm plastic scintillators, coupled to Philips XP2020 photomultiplier tubes. The resolution of the apparatus was about 230 ps. All the measurements were performed at room temperature. Each spectrum contained about 10^7 counts. Deconvolutions were carried out through the computer code LT [8], with a suitable correction for the positrons annihilated in the Kapton.

3. Results and discussion

3.1. Thermal analysis

Table 1 reports some physical characteristics of the polyethers and polyisocyanurates used in this work as base materials. It is relevant to underline that the two polyols have the same number average molecular weight M_n, but the PFPE has a shorter chain. In fact the average number of carbon and oxygen atoms constituting the molecular body is 41.4 in the case of the PFPE against 51.7 for PPG, due to the higher formula weight of the repeat unit of the fluorinated polyether. The determined equivalent weights of the isocyanurate trimers is higher than those of the corresponding diisocianate monomers (222 vs. 245 for IPDI, 168 vs. 183 for HDI), suggesting that these products are more

Table 1
Characteristics of the polyether and polyisocyanurate starting materials

Macromer type	Functionality	M_n	Equivalent weight (g/eq)	T_g (K)	ΔC_p (J g^{-1} K)	Density 20°C (g ml^{-1})
PPG	2 — OH	1000	500	203	0.63	1.00
PFPE	1.98 — OH	1030	516	188	0.28	1.76
HDI trimer	>3 — NCO	n.d.	183	206 (265)[a]	0.54 (0.63)[a]	1.16
IPDI trimer	>3 — NCO	n.d.	245	343 (365)[a]	0.30 (0.41)[a]	1.15

[a] Values after endcapping with methanol into methyl-urethane derivatives.

precisely polyisocyanurates with an average NCO functionality slightly higher than 3.

The prepolymers obtained by addition of the polyethers to the polyisocyanurates can be represented in the following way:

$(OCN)_2$-R-NHCOO-polyether-OCONH-R-$(NCO)_2$

where R is the polyisocyanurate ring bearing the hexamethylene (aliphatic) or isophorone (cycloaliphatic) radicals. The crosslinking reactions can be carried out through hydrolysis and self-condensation of NCO groups, forming urea linkages –NH–CO–NH–, or through formation of urethane linkages –O–CO–NH– after addition of the remaining part of polyether polyols (bicomponent). Details on different mechanisms of curing are reported in Ref. [2]. The resulting eight polymeric materials are therefore highly diversified as content and type of polyether phase, as well as amount of polyfunctional isocyanate macromer. This last parameter can be correlated to the density of crosslinking of the coatings.

Table 2 summarizes the main compositional features of the coatings under investigation, along with their T_g and ΔC_p values.

As already reported for PFPE copolymers [2,9], the DSC traces of the PFPE coating series always show two distinct T_g values which can be attributed to the segregation of soft fluorinated and hard urethane phases. The upper T_g values are obviously higher for the stiffer IPDI containing materials. For the PFPE-IPDI moisture cured polymer the T_g is extremely high and dependent on the thermal history of the specific sample (kinetic effects) [2]. The lower temperature T_g corresponds to very low intensity transitions. This is partially due to the small ΔC_p of perfluoropolyethers (about 0.28 J g^{-1} K [10]), but also crosslinking constraints are known to reduce heat capacity changes [11].

In the PPG series, only one glass transition temperature T_g is evident from the calorimetric analysis, without any evident phase segregation phenomena between the polyether and polyisocyanurate phases. The T_g value increases on passing from the HDI to the harder IPDI containing materials, and especially increases in the MC coatings. This last behavior can be explained by several factors: in fact the MC coatings have a higher content of high T_g isocyanurate phase, have a higher density of crosslinking (that is a lower molecular weight between crosslinks, M_c), more hydrogen bonding due to the presence of urea linkages. The behavior of T_g and ΔC_p of PPG polyurethanes can be discussed according to the well known Fox–Flory equation:

$$1/T_g = 1/T_{g1}w_1 + 1/T_{g2}w_2 \tag{1}$$

and by assuming as valid a heat capacity compositive law:

$$\Delta C_p = \Delta C_{p1}w_1 + \Delta C_{p2}w_2 \tag{2}$$

Table 2
Characteristics and composition of polyurethane coatings

Coating type	Polyether content (w/w, %)	Polyisocyanurate content (w/w, %)	T_g (K)	ΔC_p (J $^{g-1}$ K)	M_c[a]
PPG + HDI bicomponent	73.2	26.8	223	0.58	2225
PPG + HDI moisture cured	45.1	54.9	243	0.55	1100
PPG + IPDI bicomponent	67.2	32.8	228	0.48	2460
PPG + IPDI moisture cured	41.7	58.3	257	0.20	1390
PFPE + HDI bicomponent	73.8	26.2	198	0.10	2305
			241	0.18	
PFPE + HDI moisture cured	45.8	54.2	193	0.02	1115
			311	0.12	
PFPE + IPDI bicomponent	67.8	32.2	192	0.02	2510
			327	0.12	
PFPE + IPDI moisture cured	42.4	57.6	196	0.02	1400
			(393)	0.03	

[a] Molecular weight between crosslinks = mass of polymer/mols of crosslinker.

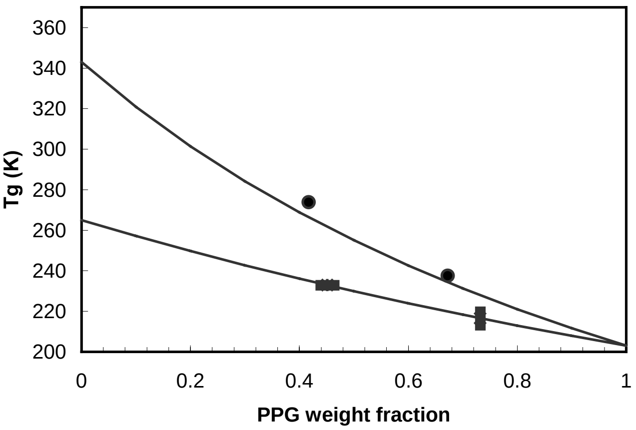

Fig. 1. Experimental glass transitions of PPG containing coatings compared to the T_g–w relation, according to the Fox–Flory equation (circles: IPDI series; squares: HDI series).

being w_1 and w_2 the weight fractions of the components. In order to take into account the effect of polymerization and crosslinking, the T_g and ΔC_p values of trimers after formation of urethane derivatives were used for the calculation of Eqs. (1) and (2) (see values reported with footnote indicator in Table 1). The experimental values are in good agreement with the calculated ones (±3–7% for glass transitions, and ±8–14% for ΔC_p) confirming the formation of 'homophase' polyurethanes, with the apparent exception of the heat capacity change of PPG-IPDI moisture cured coating. In this last case a partial phase separation of highly crosslinked polyurea structures cannot be excluded. In Fig. 1 the experimental T_g values are compared with T_g–w trend obtained according to Eq. (1).

A first clear difference between the two classes of materials can be therefore envisaged: while fluorinated polyurethanes are clearly biphasic, the corresponding structures based on polypropyleneglycol show a good compatibility between urethane and polyether macromers. The different behavior between PPG and PFPE, whose starting T_g values are rather close, has to be attributed to the extremely low solubility parameter [12] of the fluorinated polyether (5.8 (cal cm^{-3})$^{1/2}$) which causes a complete immiscibility with the polar [13] urethane moiety (ca. 10 (cal cm^{-3})$^{1/2}$). On the other hand, linear PPG based polyurethanes are known to be a one-phase system [14], because of the high solubility parameter (9.1 (cal cm^{-3})$^{1/2}$) of this polyether segment.

3.2. Positron annihilation measurements

Annihilation time spectra in the PPG series were analyzed into three components, whose lifetimes are attributed to *para*-Ps (τ_1), to free positrons (τ_2) and to *ortho*-Ps (τ_3); they are reported in Table 3. The values of τ_1 are in the range of *para*-Ps lifetimes in condensed matter [15] and the corresponding intensity I_1 is in fair agreement with one-third of I_3, as it is expected from the ratio of the statistical weights of the *para* to *ortho*-Ps sublevels [15]. Ps is generally thought to be formed in the subnanometric holes forming the free volume, and *ortho*-Ps lifetime is longer, the larger is the hole [3]. Since hole sizes are distributed around an average value, a distribution of *ortho*-Ps lifetimes in the timing spectrum is expected. Accordingly, in our analyses we required the longest lifetime component to be distributed (the LT code allows the introduction in a time annihilation spectrum of a lifetime distribution for one or more components), whilst the shorter components were assumed to decay as simple exponentials. In Table 1 τ_3 is the centroid of the lifetime distribution and σ is its second moment. Since nanohole sizes significantly expand for $T > T_g$, τ_3 should increase when the difference $|T_{room} - T_g|$ increases; indeed, our data confirm this contention. The ratio σ/τ_3 is stable for the investigated PPG series; also the intensity I_3 does not show significant variations with the composition of the samples.

Table 3 also displays the lifetime spectra obtained in PFPE series. The most important feature is that it is not possible to analyze them in only three components, even by allowing the longest one to be a distribution of lifetimes; in fact, the χ^2 was unacceptable. Therefore, the PFPE spectra were analyzed into four components, with the possibility for the longest one (τ_4) to be a lifetime distribution; interpretation of the shorter components is the same of that previously given for PPG. τ_3 and τ_4 are in the range 1.1–1.3 and 4–5 ns, respectively; that is, much longer than the free positron lifetimes. Therefore, we interpret the two longest components (lifetimes τ_3 and τ_4) in terms of two distinct Ps states, decaying from different regions, which could

Table 3
Positron data for the investigated polymers

Sample	τ_1 (ns)	I_1 (%)	τ_2 (ns)	I_2 (%)	τ_3 (ns)	I_3 (%)	τ_4 (ns)	I_4 (%)	σ (ns)	χ^2	Polyisocyanurate content (w/w, %)	R_3 (nm)	ΔR_3 (nm)	R_4 (nm)	ΔR_4 (nm)
PPG + HDI bicomponent	0.12	12.5	0.35	52.2	2.42	35.3	–	–	0.80	1.00	26.8	0.32	0.06	–	–
PPG + HDI MC	0.11	12.2	0.33	52.7	2.08	35.1	–	–	0.68	0.99	54.9	0.30	0.06	–	–
PPG + IPDI bicomp.	0.13	12.8	0.34	48.2	2.28	39.0	–	–	0.79	1.06	32.8	0.31	0.06	–	–
PPG + IPDI MC	0.14	12.6	0.35	48.9	1.95	38.5	–	–	0.68	1.02	58.3	0.28	0.06	–	–
PFPE + HDI bicomponent	0.12	10.4	0.38	59.4	1.31	6.8	5.19	23.3	0.77	1.01	26.2	0.21	–	0.49	0.03
PFPE + HDI MC	0.14	12.1	0.36	54.6	1.26	11.1	4.46	22.3	1.09	1.04	54.2	0.21	–	0.46	0.05
PFPE + IPDI bicomponent	0.13	11.1	0.36	55.1	1.13	7.6	4.49	26.1	0.80	1.05	32.2	0.19	–	0.46	0.04
PFPE + IPDI MC	0.12	9.9	0.37	57.3	1.18	9.6	4.04	23.2	0.90	1.03	57.6	0.20	–	0.43	0.05

correspond to the two phases segregated in the coating. This interpretation is supported by the fact that each phase shows its own glass transition: the fluorinated phase is characterized by low T_g in the investigated structures; *ortho*-Ps trapped in the corresponding nanoholes displays a lifetime between 4 and 5 ns, which seems to be slightly higher for the bicomponent polymer than for the moisture cured one. On the other hand, lifetime τ_3 corresponds to the other Ps state which is associated to the urethane phase. Actually, this Ps state very likely has a lifetime distribution, but statistics of our spectra did not allow us to reliably extract a distribution for this component. For this reason only the centroid τ_3 is displayed in Table 3. Although the total *ortho*-Ps intensity $I_3 + I_4$ is quite constant, as in PPG coatings, I_3 shows a correlation with the content of poly-isocyanurate, since it increases for the moisture cured coatings.

From our data we can obtain information on the size R of the nanoholes using the following, semiempirical relationship [4,16]:

$$\tau^{-1} = \lambda_0\left[1 - \frac{R}{R_0} + \frac{1}{2\pi}\sin\left(2\pi\frac{R}{R_0}\right)\right] \qquad (3)$$

where $\lambda_0 = 2\ \text{ns}^{-1}$ and τ(ns) is the *ortho*-Ps lifetime. Eq. (3) is obtained by modeling Ps as trapped in a spherical void having a potential well with infinite barrier height; the radius $R_0 = R + \Delta R$, ΔR being an empirical parameter which describes the penetration of Ps wave function into the bulk (it results $\Delta R = 0.166$ nm [4]). The electron density is assumed to be zero for $r < R$ and constant for $r > R$. The values of R for the investigated structures are shown in Table 3; they should be interpreted as a rough estimate of the actual sizes, since real voids are not spherical, but irregularly shaped. According to our results the smallest nanoholes (0.19–0.21 nm) are found in the hard domains of PFPE structures; conversely, the fluorinated phase hosts the larger holes (0.43–0.49 nm). Free volumes in PPG (0.28–0.32 nm) are in an intermediate position.

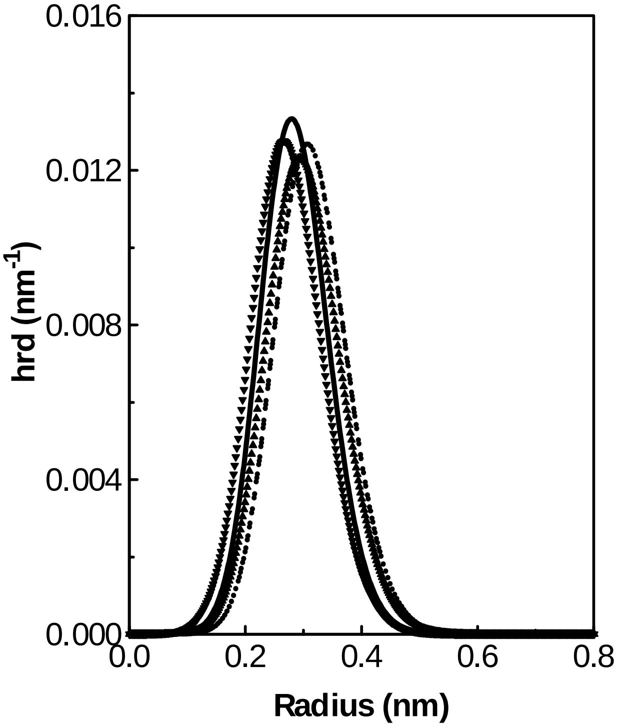

Fig. 2. Hole radius distribution (hrd) for the investigated polypropyleneglycol (dashed line: PPG + HDI bicomponent; continuous line: PPG + HDI moisture cured; up triangles: PPG + IPDI bicomponent; down triangles: PPG + IPDI moisture cured).

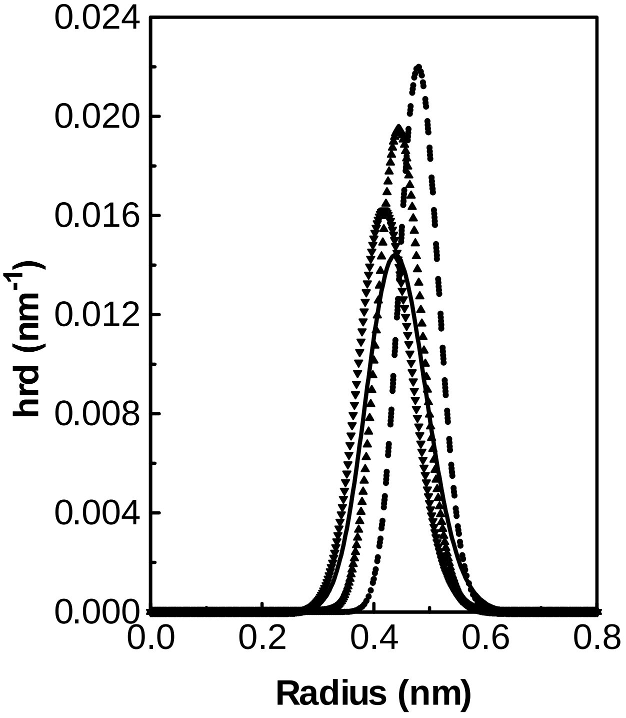

Fig. 3. Hole radius distribution (hdr) for the investigated perfluoropolyether macrodiols (dashed line: PFPE + HDI bicomponent; continuous line: PFPE + HDI moisture cured; up triangles: PFPE + IPDI bicomponent; down triangles: PFPE + IPDI moisture cured).

At last, it is possible to transform the lifetime distribution into the probability density function of the nanoholes sizes [17]; the results are shown in Figs. 2 and 3.

4. Conclusions

In this work, we discussed some correlations among macroscopic features of some crosslinked fluorinated and non-fluorinated polyether-urethanes and their free volume properties as probed by positron annihilation lifetime spectroscopy. The most important result is that this technique is sensitive to the phase segregation, since one or two distinct lifetime distributions are found in the structures, according to the presence of one or two segregated phases in the polymer network.

Furthermore, *ortho*-Ps parameters are influenced by the properties of the polymers: lifetimes are related to the value of the glass transition temperature and I_3 in the fluorinated polyurethanes is sensitive to the polyisocyanurate content.

At last, we deduced the size distributions — in spherical approximation — of the nanoholes present in the materials.

References

[1] Wicks ZW, Jones FN, Pappas SP. Organic coatings: science and technology, vol. I. New York: Wiley, 1992. Chapter 12.

[2] Turri S, Scicchitano M, Marchetti R, Sanguineti A. In: Hougham G, Cassidy PE, Johns K, Davidson T, editors. Fluoropolymers 2: properties. New York: Kluwer Academic Science, 1999. p. 145–69.

[3] Jean YC. In: Dupasquier A, Mills Jr. AP, editors. Positron spectroscopy of solids. Amsterdam: IOS Press, 1995. p. 563–80.

[4] Eldrup M, Lightbody D, Sherwood NJ. Chem Phys 1981;63:51.

[5] ASTM D2572-80.

[6] Turri S, Barchiesi E, Levi M. Macromolecules 1995;28:7271.

[7] Schrader DM, Jean YC. In: Schrader DM, Jean YC, editors. Introduction, in positron and positronium chemistry. Amsterdam: Elsevier, 1988. p. 13.

[8] Kansy J. Nucl Instr Methods A 1996;374:235.

[9] Levi M, Turri S. J Polym Sci, Part A: Polym Chem 1998;36:939.

[10] Tonelli C, Bassi M, Ajroldi G. J Polym Sci, Part B: Polym Phys 1999;3:1609.

[11] ten Brinke G, Karasz FE, Ellis TS. Macromolecules 1983;16:244.

[12] Marchionni G, Ajroldi G, Pezzin G. In: Aggarwal SL, Russo S, editors. Comprehensive polymer science. New York: Pergamon Press, 1996. p. 360. 2nd Supplement.

[13] Burrel H. In: Brandrup J, Immergut EH, editors. Polymer handbook, 2nd ed. New York: Wiley, 1975. p. IV-358.

[14] Camberlin Y, Pascault JP. J Polym Sci, Part B: Polym Phys 1984; 22:1835.

[15] Consolati G, Quasso F. Appl Phys 1991;A52:295–8.

[16] Tao SJ. J Chem Phys 1972;56:5499.

[17] Gregory RB. J Appl Phys 1991;70:4665.